Available online at www.sciencedirect.com
ScienceDirect
Electrochemistry Communications 10 (2008) 668–672
electrochemistry communications
www.elsevier.com/locate/elecom

Oxygen reduction behavior of RuO_2/Ti, IrO_2/Ti and Ir*M* (*M*: Ru, Mo, W, V) O_x/Ti binary oxide electrodes in a sulfuric acid solution

Yoshio Takasu *, Norihiro Yoshinaga, Wataru Sugimoto

Department of Fine Materials Engineering, Faculty of Textile Science and Technology, Shinshu University, 3-15-1 Tokida, Ueda 386-8567, Japan

Received 9 January 2008; received in revised form 11 February 2008; accepted 11 February 2008
Available online 15 February 2008

Abstract

Some oxide catalysts, such as RuO_2/Ti, IrO_2/Ti and Ir*M*(*M*: Ru, Mo, W, V)O_x/Ti binary oxide electrodes, were prepared by using a dip-coating method on a Ti substrate. Their catalytic behavior for the oxygen reduction reaction (ORR) was evaluated by cyclic voltammetry in 0.5 M H_2SO_4 at 60 °C. These catalysts were found to exhibit considerably high activity, and the most active one among them was $Ir_{0.6}V_{0.4}O_2$/Ti prepared at 450 °C, showing onset potential for the ORR at about 0.86 V–0.90 (vs RHE).

Keywords: Iridium oxide; Oxygen reduction reaction; Electrocatalyst; Fuel cell; Ruthenium oxide

1. Introduction

Although the typical cathode catalysts used for Polymer Electrolyte Fuel Cells (PEFCs) are presently Pt-based alloys due to their high oxygen reduction activity, platinum is a highly expensive material. The development of catalysts to replace platinum, including oxides [1–3], carbides [4,5], and metal complexes [6,7], etc., has widely been examined by many research groups up to the present. Since iridium oxide is a typical material that resists corrosion in acidic solutions and is one of the outstanding electrocatalysts for oxygen evolution, IrO_2–Ta_2O_5/Ti electrodes [8,9] have been used as oxygen-evolving anodes in the industrial electro-plating process, and the IrO_2–RuO_2–TiO_2/Ti ternary oxide electrode is widely used as the Dimensionally Stable Anode (DSA®) catalyst-electrode in the electrolysis process for chlorine production in chlor-alkali industries [10]. Although basic investigations on the ORRs of iridium metal and compounds in acidic solutions have been published [11–14], reports on crystalline iridium oxide in acidic solutions have been scarce to date [15].

This study presents a fundamental investigation of the development of non-Pt catalyst cathodes for PEFCs, using RuO_2, IrO_2 and IrO_2-based binary oxides coated on a Ti plate substrate.

2. Experimental

Individual oxides: RuO_2, IrO_2 and equimolar binary oxides of IrO_2 mixed with either MoO_x, VO_x or TiO_2 were prepared on Ti substrates by a dip-coating method using butanolic solutions of metal salts: $RuCl_3$, $IrCl_3$, $MoCl_5$, $VOCl_3$ and C_4H_9O–[Ti$(OC_4H_9)_2O]_4$–C_4H_9O. Calcination of the dip-coated salts was conducted at 450 °C in air. The dipping–drying–calcination procedure was repeated 5 times in order to prepare electrodes showing reproducible performance. These oxide electrodes are denoted as the RuO_2/Ti, IrO_2/Ti, IrRu(1:1)O_x, IrMo(1:1)O_x/Ti, IrV(1:1)O_x/Ti and IrTi(1:1)O_x/Ti electrodes. The loading amount of IrO_2 coated on the Ti substrate of the IrO_2/Ti electrode determined with a microbalance was about 250 μg/cm^2.

* Corresponding author. Tel.: +81 268 21 5451; fax: +81 268 22 5458.
E-mail address: ytakasu@shinshu-u.ac.jp (Y. Takasu).

1388-2481/$ - see front matter © 2008 Elsevier B.V. All rights reserved.
doi:10.1016/j.elecom.2008.02.014

The ORR activity of these oxide electrodes was evaluated by cyclic voltammetry (CV) in 0.5 M H_2SO_4 using a beaker-type electrolytic cell in a stationary state at 60 °C. A carbon felt, rather than Pt, was used as the counter-electrode in order to avoid the deposition of Pt onto the test electrode through dissolution. Although an Ag/AgCl reference electrode was used, the electrode potential is presented vs RHE. A Luggin capillary faced the working electrode at a distance of 2 mm. All electrode potentials referred to RHE(t) scale, corrected for the effects of temperature. For the ORR experiment, nitrogen gas or oxygen gas was bubbled into 0.5 M H_2SO_4 solution at 60 °C.

3. Results and discussion

Fig. 1 shows CVs of the RuO_2/Ti, IrO_2/Ti, IrRu(1:1)O_x, IrMo(1:1)O_x/Ti, IrV(1:1)O_x/Ti and IrTi(1:1)O_x/Ti electrodes in N_2-saturated 0.5 M H_2SO_4 (dotted lines) and in O_2-saturated 0.5 M H_2SO_4 (solid lines). During both potential scans (anodic and cathodic potential sweeps), an additional cathodic current was observed for those CVs measured with the O_2-saturated solution than for those measured with the N_2-saturated solution. This additional cathodic current is due to the ORR on each of the oxide electrodes. The onset electrode potential, E_{ORR}, for the ORR is defined by two ways in this paper. The first one is the potential where the additional cathodic current begins to be observed on the voltammogram, $E_{ORR\text{-}0}$, and the second one is the potential where the additional cathodic current attained to 20 μA/cm^2-(geometric), $E_{ORR\text{-}20}$. The onset electrode potentials for the ORR on RuO_2/Ti, IrO_2/Ti, IrRu(1:1)O_x/Ti, IrMo(1:1)O_x/Ti, IrV(1:1)O_x/Ti and IrTi(1:1)O_x/Ti are listed in Table 1. Among these electrodes, the IrV(1:1)O_x/Ti electrode showed the highest activity for the ORR.

Fig. 2 shows ORR cathodic current curves for these electrodes which were obtained by subtracting the voltammogram of the O_2-saturated solution during the cathodic scan from that of the N_2-saturated one. Since the voltammetry was carried out in a stationary state and the effective surface areas of these oxide electrodes have not been evaluated, comparison of the ORR current density among these electrodes must be performed carefully. The apparent ORR current density per geometric surface area of these electrodes shows that the IrV(1:1)O_x/Ti electrode had the highest activity among these electrodes. In the case of the IrO_2-containing binary oxide electrodes, IrO_2 is resistant to corrosion in the electrolytic solution, but the other oxide

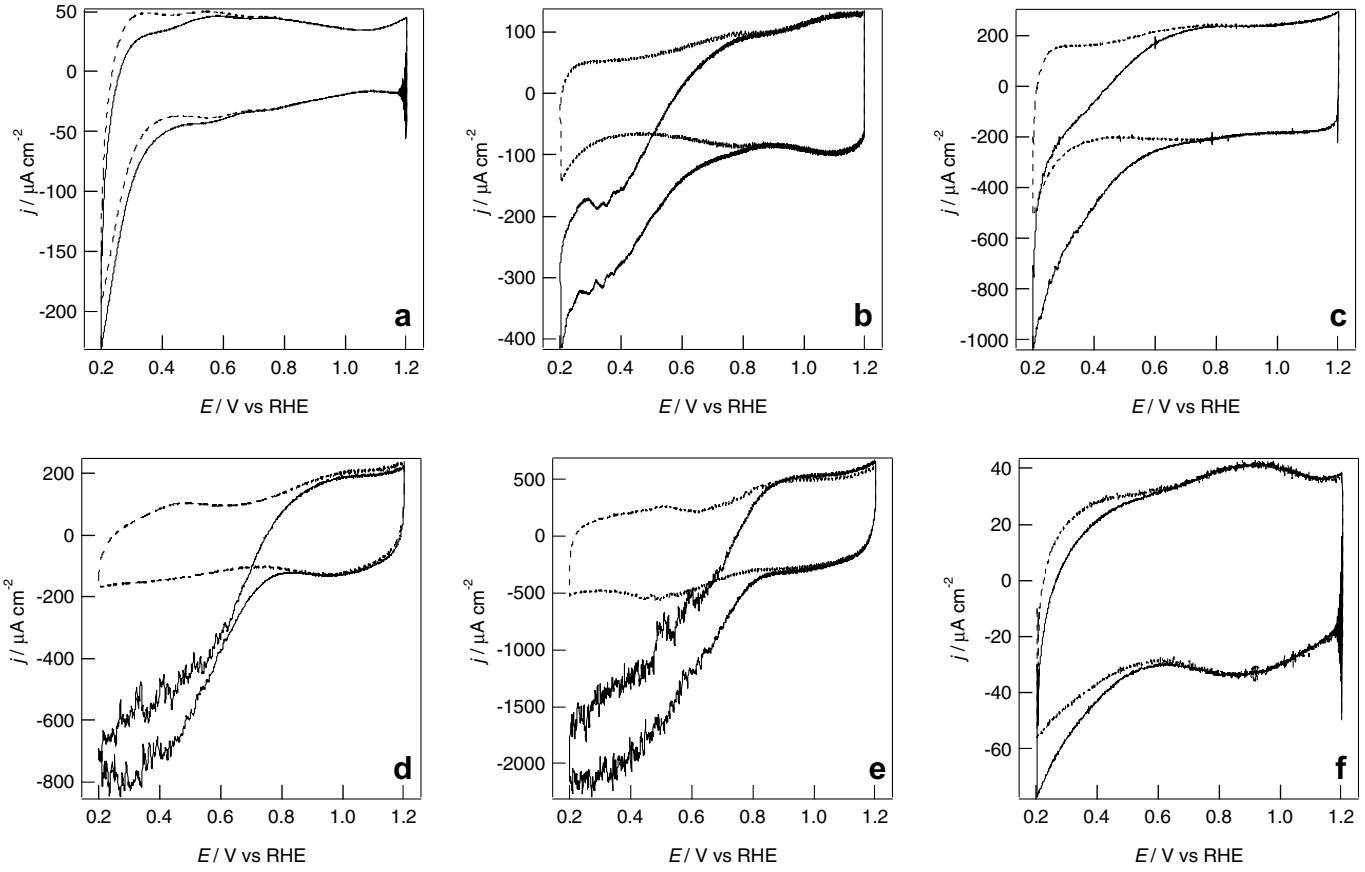

Fig. 1. Cyclic voltammograms of the rutile-type oxide electrodes prepared using the dip-coating method at 450 °C. Electrodes: a) RuO_2/Ti, b) IrO_2/Ti, c) IrRu(1:1)O_x/Ti, d) IrMo(1:1)O_x/Ti, e) IrV(1:1)O_x/Ti, f) IrTi(1:1)O_x/Ti. The broken lines indicate measurement in N_2-saturated 0.5 M H_2SO_4 and the solid lines indicate O_2-saturated 0.5 M H_2SO_4 (60 °C, 5 mV/s). The current density is presented as current per geometric surface area of the electrodes.

Table 1
The onset electrode potentials for the ORR on various electrodes

	RuO_2/Ti	IrO_2/Ti	$IrRu(1:1)O_x$/Ti	$IrMo(1:1)O_x$/Ti	$IrV(1:1)O_x$/Ti	$IrTi(1:1)O_x$/Ti
$E_{ORR\text{-}0}$/V(vs RHE)	0.72	0.84	0.78	0.87	0.90	0.75
$E_{ORR\text{-}20}$/V(vs RHE)	0.21	0.74	0.67	0.79	0.86	0.32

The definition of $E_{ORR\text{-}0}$ and $E_{ORR\text{-}20}$ is described in the text.

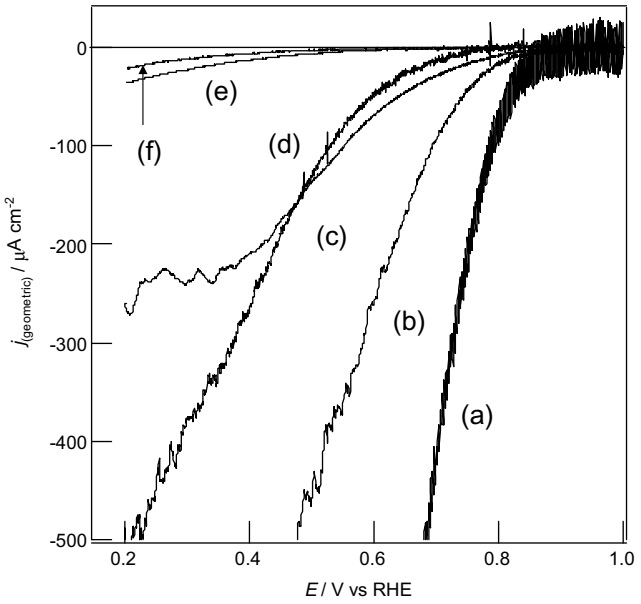

Fig. 2. The ORR-current curves of various rutile-type RuO_2/Ti, IrO_2/Ti and $IrMO_x$/Ti (*M*: metal) electrodes measured in 0.5 M H_2SO_4 (60 °C, 5 mV/s). Electrodes: a) $IrV(1:1)O_x$/Ti, b) $IrMo(1:1)O_x$/Ti, c) $IrRu(1:1)O_x$/Ti, d) IrO_2/Ti, e) RuO_2/Ti, f) $IrTi(1:1)O_x$/Ti.

species, particularly V_2O_5, were not incorporated into the IrO_2-lattice and may be unstable. Therefore, the binary oxide electrodes were treated 50 times with a potential sweeping treatment between 0.2 and 1.2 V (vs RHE) at 50 mV/s to remove unstable species in H_2SO_4 before electrochemical measurement. Four candidate reasons are proposed for this enhancement by the addition of the other elements to IrO_2: (a) an increase in the effective surface area of the oxide electrodes, (b) the incorporation of new active sites with the doped element, (c) the modification of the electronic state of Ir ions in the oxide layer and (d) an increase in the lattice defects in the oxide electrodes.

Cyclic voltammograms for the ORR on $Ir_{1-x}VO_x$/Ti electrodes prepared with various vanadium contents at 450 °C are shown in Fig. 3. The content shown in the voltammograms indicates the value determined by energy dispersive X-ray analysis (EDX), which was carried out after electrochemical measurement. The maximum $E_{ORR\text{-}20}$ was found to be 0.86 V (vs RHE) for the $Ir_{0.6}V_{0.4}O_2$/Ti electrode, and $E_{ORR\text{-}20}$ on $Ir_{0.7}V_{0.3}O_2$/Ti and $Ir_{0.5}V_{0.5}O_2$/Ti were 0.80 V and 0.68 V (vs RHE), respectively.

As shown by the high-resolution scanning electron microscopy of the $Ir_{0.6}V_{0.4}O_2$/Ti electrode before (Fig. 4a) and after (Fig. 4b) the electrochemical polarization for the measurement of the characteristics of the ORR, their surfaces were composed of fine oxide particles a few nanometers in diameter. The vanadium content of this electrode determined by EDX after the electrochemical polarization was the same as that determined before polarization, when the electrode was exposed 50 times beforehand to the electrochemical potential sweep treatment

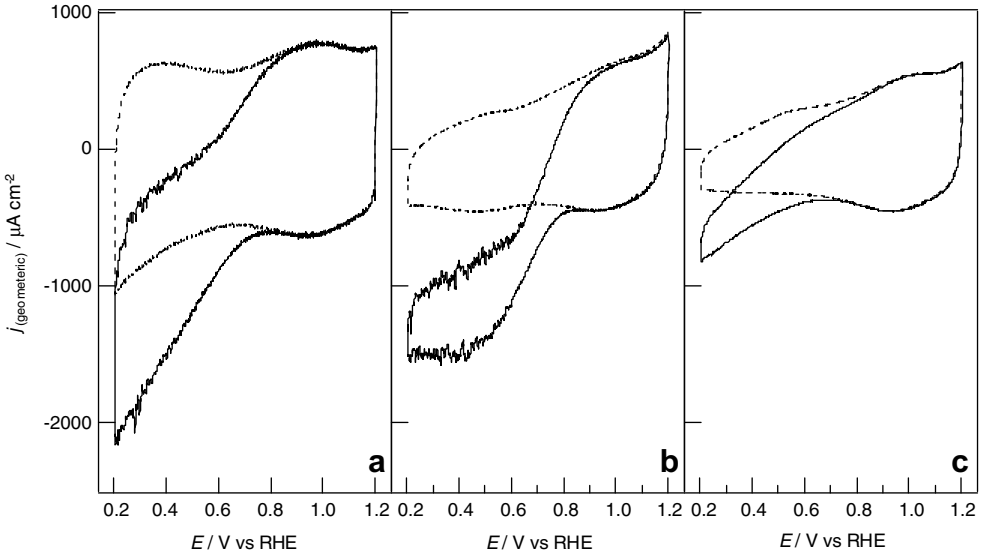

Fig. 3. Cyclic voltammograms for the ORR on $Ir_{1-x}VO_x$/Ti electrodes with various vanadium contents measured in 0.5 M H_2SO_4 (60 °C, 5 mV/s). Electrodes: a) $Ir_{0.7}V_{0.3}O_2$/Ti, b) $Ir_{0.6}V_{0.4}O_2$/Ti, c) $Ir_{0.5}V_{0.5}O_2$/Ti. The vanadium content was determined by EDX after electrochemical measurement.

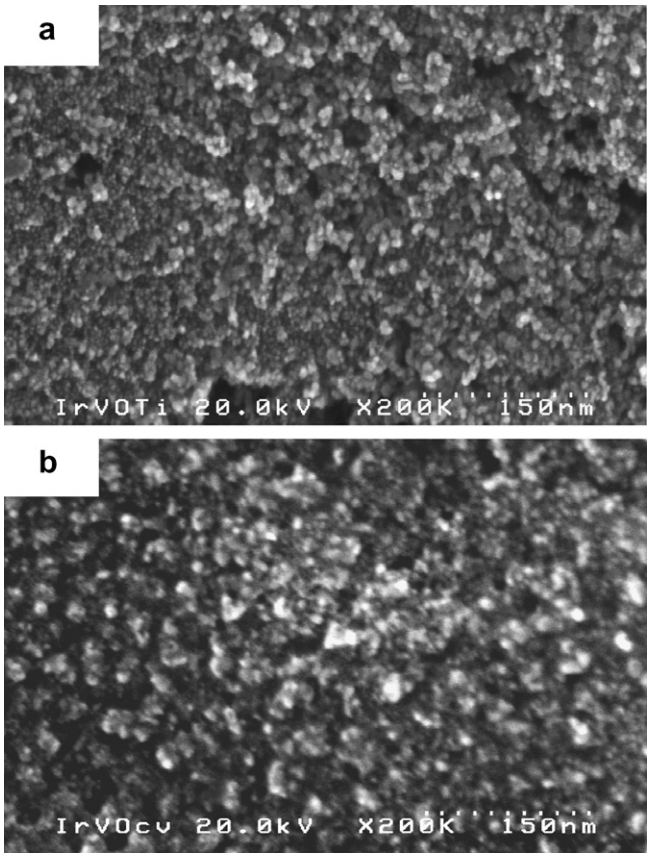

Fig. 4. Typical SEM images of the $Ir_{0.6}V_{0.4}O_2$/Ti electrode prepared at 450 °C using the dip-coating method followed by the potential sweeping treatment between 0.2 and 1.2 V (vs RHE) at 50 mV/s to remove unstable species in H_2SO_4. The upper image (a) shows the surface before the electrochemical polarization for the measurement of the ORR characteristics, and the lower one (b) shows the surface after the electrochemical polarization for the ORR.

between 0.02 and 1.2 V (vs RHE) at 50 mV/s. No appreciable changes in the rutile-type X-ray diffraction (XRD) patterns of these electrodes were observed even after electrochemical measurement. Vanadium signals were detected by an X-ray photoelectron spectroscopy (XPS) performed on electrodes exposed to electrochemical measurement, while the quantitative determination of the composition has not yet succeeded because of the surface roughness of the electrode. It is noteworthy that the $Ir_{0.6}V_{0.4}O_2$/Ti electrode exhibited about twice the activity of a flat Pt plate electrode at 0.8 V (vs RHE) when the current density for the ORR was evaluated from the geometric surface area (Fig. 5). This oxide electrode may have a roughness factor of several decades; therefore, the actual effective surface area of this porous oxide electrocatalyst requires evaluation.

Pauporté and his co-workers investigated the valency of iridium ions in sputtered iridium oxide film by X-ray absorption spectroscopy (XAS) at the L_3 edge of iridium atoms in 1 M H_2SO_4, and determined the valency of iridium to be 3 to 3.85 when the potential varied from −0.2 to +1 V (vs SCE) [16]. If we adapt their results to our findings, the valency of the iridium ion at 0.90 V (vs RHE), the E_{ORR} of the $Ir_{0.6}V_{0.4}O_2$/Ti electrode heat-treated at 450 °C, corresponds to ca. 3.78. The effect of vanadium ion incorporated into the rutile-type structure on the valency of iridium ions should be determined in a future work.

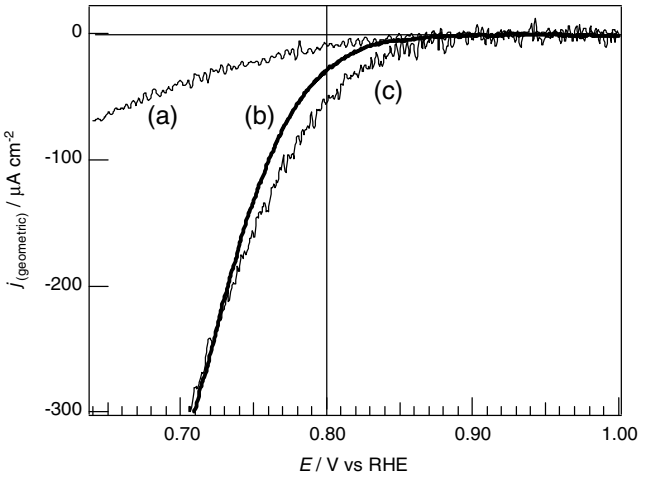

Fig. 5. The ORR-current curves of three different electrodes measured in 0.5 M H_2SO_4 (60 °C, 5 mV/s). Electrodes: a) IrO_2/Ti, b) Pt plate, c) $Ir_{0.6}V_{0.4}O_2$/Ti. The vanadium content was determined by EDX after electrochemical measurement.

4. Conclusion

In this investigation, dip-coated RuO_2/Ti, IrO_2/Ti and Ir*M* (*M*: Ru, Mo, W, V) O_x/Ti binary oxide electrodes (Ir: =1:1 in molar ratio) were prepared and their ORR activity was evaluated in 0.5 M H_2SO_4 solution at 60 °C. Among these electrodes, the IrV(1:1)O_2/Ti electrode, in nominal content, showed the highest E_{ORR} value. The vanadium ions incorporated into the rutile-type structure of iridium oxide were stable even after 50 electrochemical potential sweeps between 0.2 and 1.2 V (vs RHE) at 50 mV/s. The examination of the vanadium content of the $Ir_{1-x}VO_x$/Ti electrodes with regard to the ORR activity revealed that the $Ir_{0.6}V_{0.4}O_2$/Ti electrode, real content, is the most active for the ORR, with an onset potential for the $E_{ORR\text{-}20}$ of 0.86 V (vs RHE).

Acknowledgements

This work was supported in part by the "Polymer Electrolyte Fuel Cell Program; Development of Next Generation Technology" from the New Energy and Industrial Technology Development Organization (NEDO) of Japan.

References

[1] B. Wang, J. Power Sources 152 (2005) 15.
[2] J.-H. Kim, A. Ishihara, S. Mitsushima, N. Kamiya, K.-I. Ota, Electrochim. Acta 52 (2007) 2492.
[3] J. Prakash, D.A. Tryk, W. Aldred, E.B. Yeager, J. Appl. Electrochem. 29 (1999) 1463.

[4] F. Mazza, S. Trassatti, J. Electrochem. Soc. 110 (1963) 847.
[5] K. Lee, A. Ishihara, S. Mitsushima, N. Kamiya, K.-I. Ota, Electrochim. Acta 49 (2004) 3479.
[6] E. Claud, T. Addou, J.-M. Latour, P. Aldebert, J. Appl. Electrochem. 28 (1998) 57.
[7] J.P. Collman, P.S. Wagenknecht, J.E. Hutchison, Angew. Chem. Int. Ed. Engl. 33 (1994) 1537.
[8] J. Rolewicz, Ch. Comminellis, E. Plattner, J. Hinden, Chimia 42 (1988) 75.
[9] J. Rolewicz, Ch. Comminellis, E. Plattner, J. Hinden, Electrochim. Acta 33 (1988) 573.
[10] K. Kameyama, K. Tsukada, K. Yahikozawa, Y. Takasu, J. Electrochem. Soc. 141 (1994) 643.
[11] D.S. Gnanamuthu, J.V. Petrocelli, J. Electrochem. Soc. 114 (1967) 1036.
[12] A.J. Appleby, J. Electroanal. Chem. 27 (1970) 325.
[13] K. Lee, L. Zhang, J. Zhang, J. Power Sources 165 (2007) 108.
[14] K. Lee, L. Zhang, J. Zhang, J. Power Sources 170 (2007) 291.
[15] Y. Takasu, W. Sugimoto, M. Yoshitake, Electrochemistry 75 (2007) 105.
[16] T. Pauporte, D. Aberdam, J.-L. Hazenmann, R. Faure, R. Durand, J. Electroanal. Chem. 465 (1999) 88.